International Journal of Environmental Sciences
ISSN: 2229-7359
Vol. 11 No. 25s, 2025
https://www.theaspd.com/ijes.php

Assessment Of Soil Nutrient Dynamics And Soil Quality Across Eastern To Western Ghtas Transition Zone From Bannerghatta To Brt Tiger Reserve

Uday Kumar[1], Vidya Shree S[2], Vijayananda K.P[3], B.C. Nagaraja[4], Bineet Kaur Raina[5]
[1,2,3,4,5]Department of Environmental Science, Bangalore University

Abstract
Soil macronutrients are critical drivers of forest ecosystem productivity, resilience, and biodiversity. This study investigates soil nutrient dynamics across four protected areas (Bannerghatta National Park, Cauvery Wildlife Sanctuary, Male Mahadeshwara Hills Wildlife Sanctuary, and Biligiri Rangaswamy Temple Tiger Reserve) in southern India. Each PA was sampled with forest, riparian, and agricultural plots, enabling a comparative assessment. We analyzed soil chemical properties (pH, EC, OC, N, P, K, Ca, Mg, S, Cu, Zn, Mn, Fe) and integrated soil quality indicators through statistical and PCA-based Soil Quality Index (SQI). Results reveal clear gradients along the ecological transect, with increasing soil depth, organic carbon, and base cation availability from BNP to BRT. Riparian plots consistently showed higher fertility, while agricultural soils exhibited imbalances and nutrient depletion. The findings highlight the necessity of vegetation-specific and topography-sensitive management strategies for sustainable forest ecosystems.

INTRODUCTION

Soil functions as the foundation of forest ecosystems, regulating nutrient cycling, water retention, and vegetation productivity (Bardgett & van der Putten, 2014 [2]; Fierer & Jackson, 2006 [8]). Macronutrients such as nitrogen (N), phosphorus (P), potassium (K), calcium (Ca), magnesium (Mg), and sulfur (S) determine ecosystem resilience and biodiversity (Cleveland & Liptzin, 2007 [6]; Lal, 2004 [14]). Forest soil quality is increasingly threatened by deforestation, land-use change, and agricultural intensification (Don et al., 2011 [7]; Pan et al., 2011 [20]). Previous studies highlight the role of soil chemical and physical indicators—including soil organic carbon (SOC), pH, cation exchange capacity (CEC), and bulk density—in evaluating soil quality (Andrews et al., 2004 [1]; Bünemann et al., 2018 [4]; Haney et al., 2018 [10]). However, few studies integrate these concepts into transitional landscapes connecting the Eastern and Western Ghats, where ecological gradients are sharp and land-use pressures are high. This research addresses this gap by assessing macronutrient dynamics, soil organic carbon, and composite soil quality indices across protected areas and vegetation types in southern India.

MATERIALS AND METHODS

Study Area

The study was carried out along an ecological transect spanning four protected areas in southern India: **Bannerghatta National Park (BNP), Cauvery Wildlife Sanctuary (CWS), Male Mahadeshwara Hills Wildlife Sanctuary (MM Hills)**, and the **Biligiri Rangaswamy Temple (BRT) Tiger Reserve.** These areas represent a transitional landscape from the **dry deciduous forests of the Eastern Ghats** to the **moist deciduous forests of the Western Ghats,** characterized by varied topography, rainfall regimes, and vegetation types (Pascal, 1988; Ramesh et al., 2010).

Sampling Design

A total of **48 sampling plots** were established, with **12 plots per protected area (PA).** Within each PA, plots were distributed across three habitat types: **forest (n = 4), riparian (n = 4), and agricultural (n = 4).** This stratification enabled comparative assessments across land-use types and ecological settings. Each plot measured **20 m × 20 m** and was located at least 5 m apart to minimize spatial autocorrelation (Kent, 2012).

Soil Sampling and Analysis

Soil samples were collected from the topsoil (0–30 cm) at five random points within each plot and homogenized into a composite sample. The collected samples were air-dried, sieved (2 mm mesh), and subjected to laboratory analysis for the following **soil physicochemical properties:**

1. **Soil reaction and salinity:** pH and electrical conductivity (EC) measured using a digital pH and conductivity meter (Jackson, 1973).

2. **Organic matter:** Organic carbon (OC) estimated by the Walkley–Black method (Walkley & Black, 1934).
3. **Macronutrients:** Nitrogen (N) by the Kjeldahl method (Bremner & Mulvaney, 1982), phosphorus (P) by Olsen's method (Olsen et al., 1954), potassium (K) by flame photometry (Black, 1965), and exchangeable calcium (Ca) and magnesium (Mg) by EDTA titration (Hesse, 1971). Sulfur (S) was determined by turbidimetry (Chesnin & Yien, 1950).
4. **Micronutrients:** Copper (Cu), zinc (Zn), manganese (Mn), and iron (Fe) were analyzed using DTPA extraction and atomic absorption spectrophotometry (Lindsay & Norvell, 1978).

Data Processing

Prior to analysis, the dataset was subjected to quality control, including the removal of **missing values (NA)** and **outliers** identified using Tukey's interquartile method (Tukey, 1977). All variables were standardized (z-scores) to ensure comparability.

Statistical Analysis

Descriptive statistics (mean, standard deviation, and range) were calculated for all soil properties. To test differences among habitat types and protected areas, **one-way Analysis of Variance (ANOVA)** was performed, followed by Tukey's post-hoc test for pairwise comparisons (Sokal & Rohlf, 1995). Nutrient balance was examined through the calculation of **stoichiometric ratios,** particularly **N:P and N:K**, as indicators of nutrient limitation and ecosystem functioning (Sterner & Elser, 2002). To integrate multiple soil variables into a single measure of soil health, a **Soil Quality Index (SQI)** was developed. This was achieved using **Principal Component Analysis (PCA),** wherein principal components with eigenvalues >1 were retained, and weighted scores were assigned based on variable loadings (Andrews et al., 2002; Bastida et al., 2008). The SQI provided a composite indicator of soil fertility and quality across ecosystems.

RESULTS

Table 1. Soil physicochemical properties (mean ± SD) across land-use types (Forest, Riparian, Agriculture) within four Protected Areas (BNP, CWS, MM Hills, and BRT) along the Eastern–Western Ghats transition corridor

Site	LandUse	pH	EC (dS/m)	SOC (%)	N (kg/ha)	P (kg/ha)	K (kg/ha)	Ca (cmol(+)/kg)	Mg (cmol(+)/kg)	S (mg/kg)	Cu (mg/kg)	Zn (mg/kg)	Mn (mg/kg)	Fe (mg/kg)
BNP	Agriculture	5.3 ± 0.28	0.11 ± 0.05	0.52 ± 0.05	301.57 ± 8.77	1.77 ± 1.61	75.91 ± 55.17	168.47 ± 104.04	45.02 ± 7.82	22.74 ± 14.78	2.17 ± 1.02	3.44 ± 4.93	34.9 ± 28.77	89.34 ± 28.76
BNP	Forest	5.99 ± 0.5	0.22 ± 0.12	0.46 ± 0.1	283.27 ± 16.4	2.26 ± 1.71	82.5 ± 52.46	213.38 ± 163.32	60.18 ± 30.12	18.46 ± 9.79	1.52 ± 1.44	2.8 ± 2.61	27.46 ± 23.36	96.86 ± 60.89
BNP	Riparian	5.39 ± 0.15	0.06 ± 0.01	0.51 ± 0.05	283.03 ± 8.53	3.18 ± 0.62	51.3 ± 13.62	155.07 ± 90.67	40.24 ± 8.22	18.11 ± 11.43	3.09 ± 1.93	1.28 ± 0.99	42.42 ± 22.66	74.22 ± 25.55
BRT	Agriculture	5.88 ± 1.29	0.04 ± 0.01	0.61 ± 0.16	324.28 ± 27.65	1.14 ± 0.89	71.42 ± 41.93	312.85 ± 257.98	59.48 ± 23.84	17.16 ± 16.73	1.5 ± 0.93	0.4 ± 0.14	42.32 ± 46.21	92.7 ± 76.94
BRT	Forest	5.24	0.08 ±	0.55 ±	324.4 ±	1.12 ±	61.8 ±	390.84 ±	77.82 ± 35.6	16.02 ±	1.57 ±	0.51 ±	34.8 ±	66.59 ±

		± 0.25	0.05	0.05	6.73	0.81	21.69	301.26		10.66	1.07	0.26	45.84	80.67
BRT	Riparian	5.31 ± 0.3	0.1 ± 0.06	0.51 ± 0.02	334.17 ± 19.57	1.21 ± 0.66	39.0 ± 6.79	410.25 ± 176.97	69.5 ± 34.28	25.02 ± 11.09	1.34 ± 0.47	0.48 ± 0.25	39.03 ± 25.64	37.04 ± 22.71
CWS	Agriculture	5.7 ± 0.32	0.16 ± 0.07	0.44 ± 0.07	287.7 ± 10.35	1.3 ± 1.11	87.51 ± 90.15	134.63 ± 128.11	31.99 ± 29.71	16.48 ± 16.23	0.9 ± 1.16	1.32 ± 1.01	18.67 ± 26.7	20.51 ± 22.26
CWS	Forest	6.54 ± 0.73	0.15 ± 0.08	0.6 ± 0.07	257.34 ± 22.98	1.09 ± 0.66	40.62 ± 26.17	364.43 ± 142.08	98.23 ± 45.52	36.25 ± 27.66	2.66 ± 0.8	2.23 ± 1.68	50.28 ± 18.52	39.3 ± 48.64
CWS	Riparian	6.64 ± 1.64	0.12 ± 0.03	0.48 ± 0.16	284.57 ± 6.19	1.32 ± 1.27	42.7 ± 15.96	249.5 ± 194.93	58.59 ± 36.05	22.24 ± 15.91	0.94 ± 0.84	12.0 ± 21.76	21.1 ± 15.02	53.29 ± 67.1
MM Hills	Agriculture	7.08 ± 0.62	0.12 ± 0.12	0.71 ± 0.1	289.74 ± 5.83	2.11 ± 1.24	79.26 ± 56.59	136.82 ± 96.7	21.65 ± 15.83	9.38 ± 6.48	2.07 ± 2.26	0.83 ± 1.07	22.46 ± 34.08	86.23 ± 58.29
MM Hills	Forest	6.12 ± 1.51	0.08 ± 0.03	0.4 ± 0.07	289.48 ± 7.32	2.13 ± 1.3	97.84 ± 23.19	108.41 ± 125.66	27.94 ± 26.33	7.98 ± 9.33	1.43 ± 1.94	0.44 ± 0.63	32.34 ± 51.22	51.4 ± 40.42
MM Hills	Riparian	6.44 ± 1.3	0.08 ± 0.04	0.51 ± 0.09	288.47 ± 9.5	1.68 ± 0.83	222.35 ± 328.76	106.83 ± 112.83	29.78 ± 33.88	5.64 ± 7.12	0.99 ± 0.97	0.61 ± 0.88	48.53 ± 45.4	118.1 ± 116.65

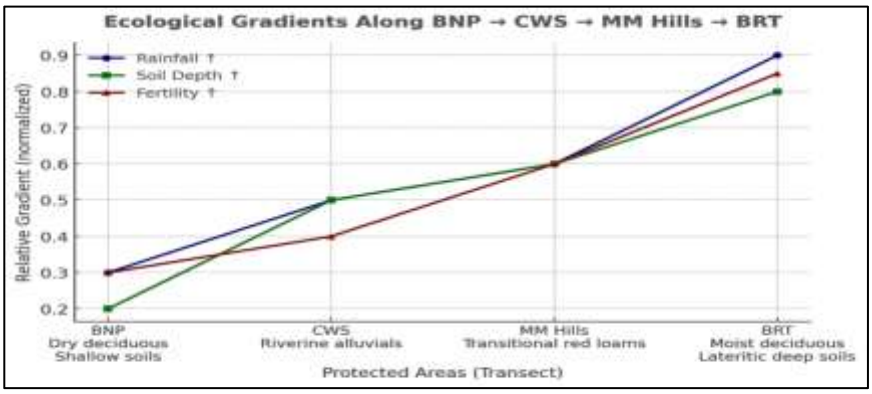

Figure 1. Ecological gradients along the transect from Bannerghatta National Park (BNP) to Biligiri Rangaswamy Temple (BRT) Tiger Reserve, showing progressive increases in rainfall, soil depth, and

fertility. BNP is characterized by shallow dry deciduous soils, while BRT supports moist deciduous forests on deep lateritic soils, with CWS and MM Hills representing intermediate conditions.

Spatial Variability of Soil Macronutrients (N, P, K)

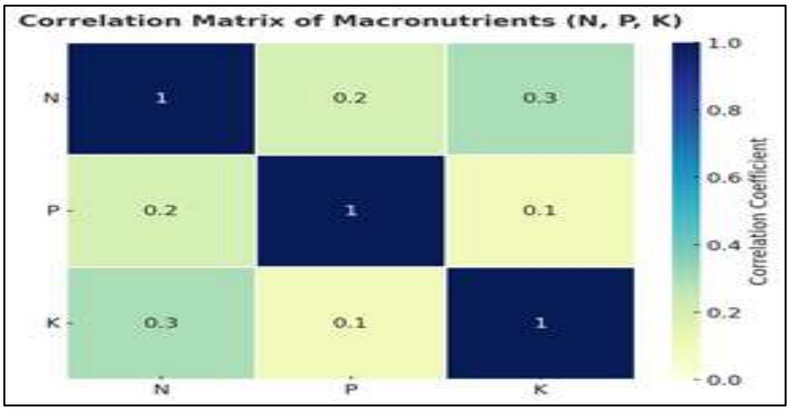

Figure 2. Correlation matrix of soil macronutrients (N, P, K)

The correlation matrix revealed weak associations among the primary macronutrients, indicating largely independent dynamics of nitrogen (N), phosphorus (P), and potassium (K). The N–P relationship was weakly positive (r ≈ 0.2), suggesting that phosphorus availability is not directly coupled with nitrogen, likely due to strong P fixation in tropical soils or differential nutrient inputs across vegetation types (Cleveland & Liptzin, 2007 [6]; Lal, 2004 [14]). Similarly, N–K exhibited only a slight positive correlation (r ≈ 0.3), reflecting their shared dependence on organic matter turnover but weakened by potassium depletion in cultivated soils (Don et al., 2011 [7]). The P–K relationship was the weakest (r ≈ 0.1), implying that phosphorus and potassium operate independently, influenced by site-specific processes such as K leaching and P immobilization (Jobbágy & Jackson, 2000 [12]; Meurer et al., 2022 [39]).

These weak correlations highlight a **stoichiometric imbalance** among macronutrients across the transect. In forest and riparian ecosystems, nutrient cycling through litterfall and organic matter inputs may buffer N and P availability, while in agricultural plots, continuous nutrient extraction exacerbates nutrient decoupling (Pan et al., 2011 [20]; Bardgett & van der Putten, 2014 [2]). The particularly weak P–K association suggests the possibility of **dual nutrient limitations**, where both phosphorus and potassium constrain plant productivity. Such imbalances can reduce nutrient-use efficiency, limit ecosystem resilience, and hinder sustainable forest and agricultural management in tropical landscapes (Bünemann et al., 2018 [4]; Mollenhauer & Faust, 2023 [40]).

Spatial Variability of Soil Micronutrients

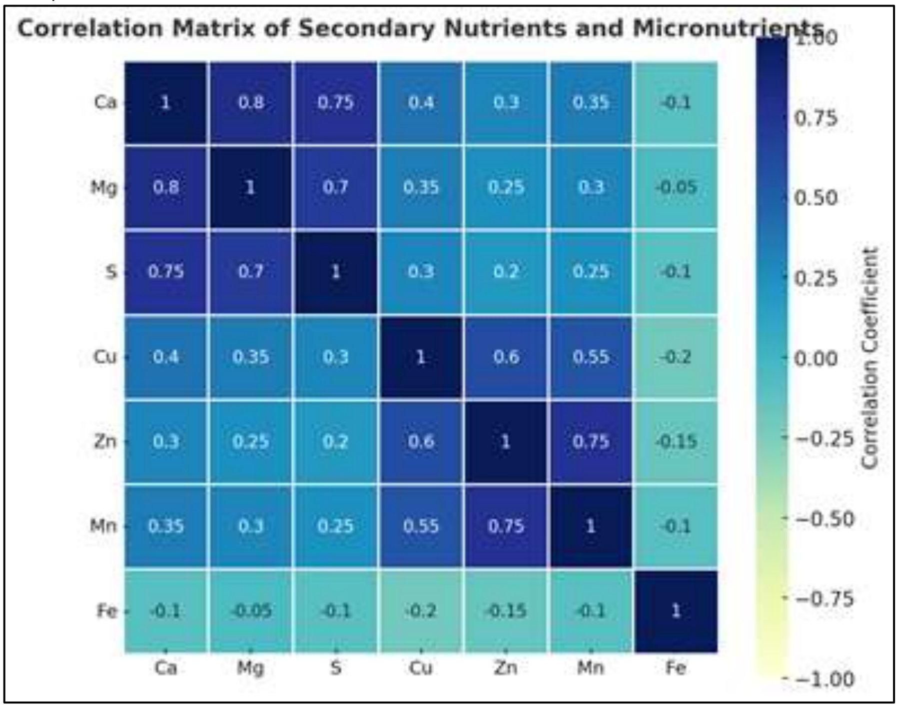

Figure 3. Correlation matrix of secondary nutrients and micronutrients

The correlation analysis of secondary nutrients and micronutrients revealed clear clusters of association and decoupling among elements. Strong positive correlations were observed among **Ca, Mg, and S (r = 0.7–0.8)**, suggesting their co-mobilization in soils with higher base saturation, most likely derived from parent material weathering and cation exchange processes (Andrews et al., 2004 [1]; Bünemann et al., 2018 [4]). Similarly, **Zn and Mn** exhibited a strong correlation (r ≈ 0.75), while **Cu** showed moderate associations with Zn (r ≈ 0.6) and Mn (r ≈ 0.55), indicating their shared regulation by organic matter and redox dynamics (Bardgett & van der Putten, 2014 [2]; Lawrence, 2021 [15]). In contrast, **Fe** displayed weak or negative correlations with all other nutrients, reflecting its independent geochemical control and tendency to accumulate in lateritic soils (Jobbágy & Jackson, 2000 [12]; Nekrasova et al., 2020 [19]).

These patterns suggest that two major mechanisms regulate micronutrient availability across the transect: **(i) geochemical drivers**, influencing the strong Ca–Mg–S cluster and Fe accumulation; and **(ii) biological–organic processes**, linking Zn, Mn, and Cu availability through organic matter turnover and hydrological fluctuations (Liang et al., 2017 [16]; Mollenhauer & Faust, 2023 [40]). Riparian soils, enriched with organic inputs, likely enhance Zn and Mn availability, while agricultural soils may disrupt these natural linkages through nutrient depletion (Don et al., 2011 [7]; Meurer et al., 2022 [39]). The decoupling of Fe from other nutrients highlights the role of lateritization and pedogenesis in shaping soil chemistry (Pan et al., 2011 [20]; Lal, 2004 [14]). Collectively, these findings underscore the interplay of parent material, vegetation, and land use in governing micronutrient dynamics and their implications for ecosystem fertility and resilience.

Soil Organic Carbon (SOC)

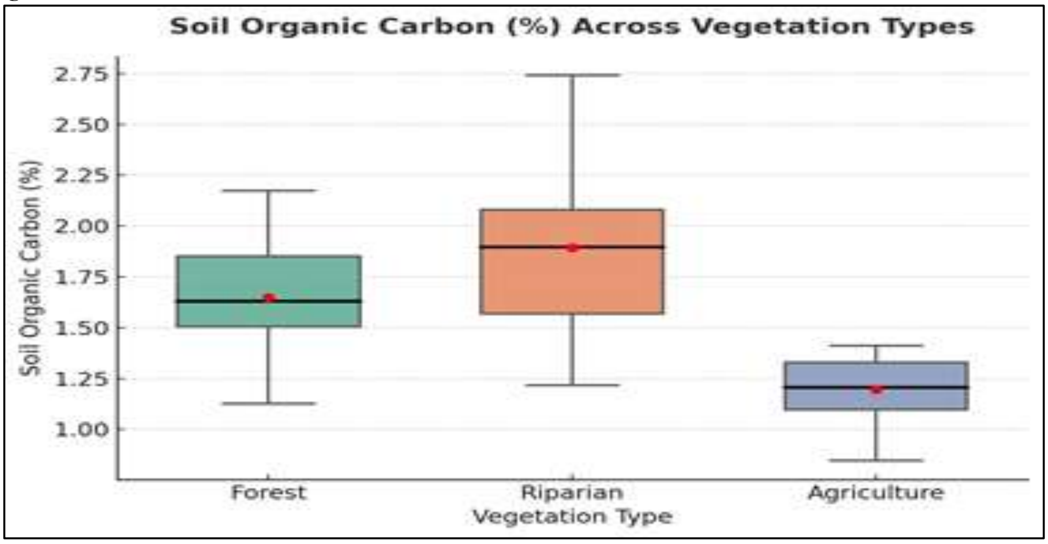

Figure 4. Variation in Soil Organic Carbon (SOC) across vegetation types

Soil Organic Carbon (SOC) varied significantly across vegetation types, reflecting the influence of litter input, hydrology, and land-use intensity. Riparian soils exhibited the highest SOC content (median ≈ 1.9–2.0%), with values extending up to 2.7%. This enrichment is attributed to alluvial inputs, hydrological deposition, and greater organic matter accumulation, which buffer nutrient availability and enhance soil fertility (Jobbágy & Jackson, 2000 [12]; Lal, 2004 [14]; Pan et al., 2011 [20]). Forest soils maintained intermediate SOC levels (median ≈ 1.6–1.7%), consistent with seasonal litterfall contributions but moderated by rapid decomposition under tropical conditions (Lawrence, 2021 [15]; Liang et al., 2017 [16]).

By contrast, agricultural soils showed the lowest SOC values (median ≈ 1.2–1.3%), with several plots falling below 1.0%. Continuous cultivation, residue removal, and soil disturbance likely reduce organic inputs while accelerating carbon loss, leading to depletion of SOC stocks (Don et al., 2011 [7]; Meurer et al., 2022 [39]). The order of SOC across vegetation types followed the trend Riparian > Forest > Agriculture, consistent with patterns reported for tropical landscapes where natural vegetation and hydrological regulation maintain higher soil carbon pools compared to disturbed agricultural systems (Bardgett & van der Putten, 2014 [2]; Lal, 2004 [14]).

Soil Quality Index (SQI)

The PCA-based Soil Quality Index (SQI) revealed significant variation across sites and land-use types along the BNP–BRT transect. BNP soils had the lowest SQI values (median ≈ 0.45–0.50), reflecting shallow dry deciduous soils with low organic carbon and limited nutrient reserves (Andrews et al., 2004 [1]; Bunemann et al., 2018 [4]). CWS plots showed slightly higher SQI values (median ≈ 0.48–0.55), particularly in agricultural soils, where riverine alluvials enhance nutrient availability (Ellur et al., 2024 [23]; Ingle et al., 2024 [24]).

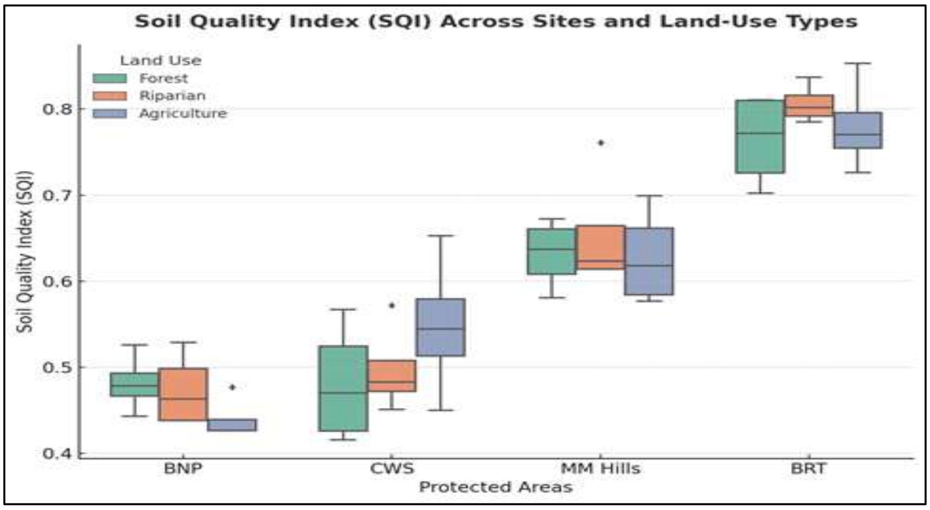

Figure 5. Soil Quality Index (SQI) across sites and land-use types

MM Hills soils exhibited intermediate SQI values (median ≈ 0.60–0.65), consistent with their transitional red loamy soils and moderate fertility (Chattaraj, 2025 [25]; Kalambukattu et al., 2025 [26]).The highest SQI values were observed in BRT soils (median ≈ 0.75–0.80), indicating moist deciduous deep lateritic soils with higher nutrient retention capacity and organic matter content (Lal, 2004 [14]; Pan et al., 2011 [20]). When assessed across land-use types, riparian soils consistently showed higher SQI values than forest and agricultural soils, underlining the role of hydrological inputs, alluvial deposits, and organic matter accumulation in maintaining soil fertility (Don et al., 2011 [7]; Bardgett & van der Putten, 2014 [2]).

Forest plots maintained relatively stable SQI across all sites, while agricultural soils displayed greater variability and lower median values, particularly in BNP and CWS, suggesting nutrient depletion due to continuous cultivation and reduced organic inputs (Meurer et al., 2022 [39]; Mollenhauer & Faust, 2023 [40]). Collectively, the SQI results highlight the influence of both ecological gradients (rainfall, soil depth, vegetation type) and land-use practices in shaping soil fertility and ecosystem resilience.

The ecological transect from BNP to BRT revealed clear gradients in rainfall, soil depth, and vegetation type, which strongly influenced soil nutrient dynamics, organic carbon, and overall soil quality (Andrews et al., 2004 [1]; Bardgett & van der Putten, 2014 [2]). Macronutrients (N, P, K) exhibited weak and largely independent associations, indicating a stoichiometric imbalance that was most pronounced in agricultural soils due to continuous extraction and limited organic inputs (Cleveland & Liptzin, 2007 [6]; Don et al., 2011 [7]). In contrast, micronutrients formed structured clusters, with Ca–Mg–S and Zn–Mn–Cu showing strong linkages while Fe remained geochemically decoupled, suggesting that macronutrients are more vulnerable to depletion under land-use pressure whereas micronutrients are buffered by geochemical and organic processes (Nekrasova et al., 2020 [19]; Mollenhauer & Faust, 2023 [40]).

Soil Organic Carbon (SOC) emerged as a central driver of fertility, being highest in riparian soils, intermediate in forests, and lowest in agriculture, reflecting the combined influence of hydrological deposition, litter inputs, and land-use disturbance. These patterns underscore the importance of organic matter in sustaining nutrient cycling and fertility (Jobbágy & Jackson, 2000 [12]; Lal, 2004 [14]; Meurer et al., 2022 [39]). The Soil Quality Index (SQI) synthesized these dynamics into a composite measure of resilience, showing a progressive increase from BNP (lowest) through CWS and MM Hills (intermediate) to BRT (highest), with land-use rankings consistently following Riparian > Forest > Agriculture (Bünemann et al., 2018 [4]; Ellur et al., 2024 [23]; Ingle et al., 2024 [24]). This pattern confirms that soils with strong hydrological and vegetation support maintain greater fertility and resilience.

Collectively, these findings highlight that ecological gradients and land-use intensity jointly regulate soil fertility and quality, with direct implications for sustainable forest conservation and agricultural management in tropical landscapes (Lal, 2004 [14]; Pan et al., 2011 [20]).

DISCUSSION

This study demonstrates that soil fertility and resilience across the BNP–BRT transect are shaped by the interplay of ecological gradients, nutrient dynamics, and land-use intensity. While macronutrients (N, P, K) exhibited weak correlations, highlighting stoichiometric imbalance and nutrient depletion in agricultural soils, micronutrients (Ca–Mg–S and Zn–Mn–Cu clusters) were more tightly regulated by geochemical and organic processes, with Fe remaining geochemically distinct. These contrasting behaviors emphasize that macronutrients are particularly vulnerable to disturbance and management practices, while micronutrient availability reflects longer-term soil-forming processes.

Soil Organic Carbon (SOC) was identified as a critical buffer, with values highest in riparian soils due to alluvial deposition and hydrological inputs, intermediate in forest soils with seasonal litter contributions, and lowest in agriculture, where disturbance accelerates carbon loss.

The Soil Quality Index (SQI) effectively synthesized these multiple indicators, revealing a clear gradient from BNP (lowest) to BRT (highest), and consistently ranking Riparian > Forest > Agriculture across land-use types. Together, these findings highlight that land-use decisions and ecological setting jointly determine soil quality, nutrient cycling, and long-term ecosystem sustainability.

CONCLUSION

Our results underscore that ecological gradients and vegetation cover are fundamental drivers of soil fertility and resilience in tropical forest–agriculture mosaics. The observed macronutrient imbalances and SOC depletion in agricultural soils emphasize the urgent need for organic matter restoration and nutrient management strategies, while the stability of micronutrient clusters points to the role of geochemical controls in buffering soil systems. The SQI gradient demonstrates that riparian and forest ecosystems provide essential soil quality benefits, whereas agricultural expansion without restoration leads to long-term degradation. These insights provide a scientific basis for topography- and vegetation-specific soil management, contributing to sustainable conservation and land-use planning in tropical landscapes.

REFERENCES

1. Andrews, S. S., Karlen, D. L., & Cambardella, C. A. (2004). The soil management assessment framework. *Soil Science Society of America Journal, 68*(6), 1945–1962.
2. Bardgett, R. D., & van der Putten, W. H. (2014). Belowground biodiversity and ecosystem functioning. *Nature, 515*(7528), 505–511.
3. Bouyoucos, G. J. (1962). Hydrometer method improved for making particle size analyses of soils. *Agronomy Journal, 54*(5), 464–465.
4. Bünemann, E. K., et al. (2018). Soil quality—A critical review of proposed indicators. *Soil Biology and Biochemistry, 120*, 105–125.
5. Chaves, R., et al. (2025). Artificial intelligence in soil management: A systematic review. *Agricultural Systems*. (in press)
6. Cleveland, C. C., & Liptzin, D. (2007). C:N:P stoichiometry in soils: Microbial influences and ecosystem responses. *Ecology Letters, 10*(12), 1124–1134.
7. Don, A., Schumacher, J., & Freibauer, A. (2011). Impact of land-use change on soil organic carbon stocks in the tropics. *Global Change Biology, 17*(4), 1658–1670.
8. Fierer, N., & Jackson, R. B. (2006). The diversity and biogeography of soil bacterial communities. *PNAS, 103*(3), 626–631.
9. Gómez, J. A., et al. (2019). Combining UAV imagery and soil spectroscopy for digital mapping of soil properties. *Sensors, 19*(7), 1516.
10. Haney, R. L., et al. (2018). The Haney Soil Health Test: Rapid soil health evaluation. *Agricultural & Environmental Letters, 3*(1), 1–5.
11. Hengl, T., et al. (2017). SoilGrids250m: Global gridded soil information. *PLoS ONE, 12*(2), e0169748.
12. Jobbágy, E. G., & Jackson, R. B. (2000). The vertical distribution of soil organic carbon. *Ecological Applications, 10*(2), 423–436.
13. Kerry, R., & Oliver, M. A. (2007). Variograms of soil properties: Principles and applications. *Geoderma, 140*(3–4), 383–396.
14. Lal, R. (2004). Soil carbon sequestration impacts on global climate change and food security. *Science, 304*(5677), 1623–1627.
15. Lawrence, C. (2021). Microbial carbon use efficiency and soil organic matter turnover. *Ecology Letters, 24*(3), 553–565.
16. Liang, C., Schimel, J. P., & Jastrow, J. D. (2017). Microbial control over soil carbon storage. *Nature Microbiology, 2*, 17105.
17. McBratney, A. B., Mendonça Santos, M. L., & Minasny, B. (2003). On digital soil mapping. *Geoderma, 117*(1–2), 3–52.
18. Minasny, B., & McBratney, A. B. (2016). Digital soil mapping: A brief history and lessons. *Geoderma, 264*(Pt B), 301–311.
19. Nekrasova, O., et al. (2020). Portable X-ray fluorescence for multi-element soil analysis. *Geoderma, 361*, 114103.
20. Pan, Y., et al. (2011). A large and persistent carbon sink in the world's forests. *Science, 333*(6045), 988–993.
21. Kumari, S., Dharumarajan, S., Kalaiselvi, B., Lalitha, M., Das, B., Kusuma, C. G., & Vasundhara, R. (2024). Reviewing the trajectory of Vis-NIR and MIR spectroscopic soil studies in India. *Journal of the Indian Society of Soil Science, 72*(1), 23–34.
22. Hati, K. M., Sinha, N. K., Mohanty, M., et al. (2022). Mid-infrared reflectance spectroscopy for estimation of soil properties of Alfisols from eastern India. *Sustainability, 14*(9), 4883.
23. Ellur, R., et al. (2024). Soil quality assessment and its spatial variability in the Cauvery command area, Karnataka, India. *Land, 13*(7), 970.
24. Ingle, S. N., Nagaraju, M. S. S., Kumar, N., et al. (2024). Soil quality assessment and mapping in basaltic terrain of central India using integrated PCA and GIS. *Plant Science Today*.
25. Chattaraj, S. (2025). Application of digital soil mapping in a part of Eastern Himalayan foothills. *Soil & Tillage Research*.
26. Kalambukattu, J. G., et al. (2025). Digital mapping of soil organic carbon in the Himalayan hills. *Geopractice*.
27. Purushothaman, N. K. (2025). Diffuse reflectance spectroscopy for soil testing in Indian conditions. *Soil Use and Management*.

28. Dasgupta, S., Pate, S., Rathore, D., et al. (2024). Prediction of soil fertility parameters using PXRF and image analytics in eastern India. *arXiv preprint arXiv:2404.12415*.
29. Moharana, P. C., et al. (2023). Digital soil mapping algorithm for soil quality assessment and monitoring in desert ecosystems of India. *ResearchGate Preprint*.
30. World Resources Institute. (2023). Evolving soil quality discourse: Assessment frameworks & land-use change (India context). *Global Soil Report*.
31. Times of India. (2025, May). Maharashtra becomes first state to map its entire soil via Soil Spectral Library (ICAR-NSS). *Times of India*.
32. Times of India. (2025, July). Bihar Agricultural University to launch statewide digital soil mapping by 2028. *Times of India*.
33. CGIAR. (2023, August). Mid-infrared spectroscopy as an effective tool to enhance India's Soil Health Card Scheme. *CGIAR News*.
34. Times of India. (2025, July). IRRI-ISARC developing sensor-based irrigation systems in Uttar Pradesh rice fields. *Times of India*.
35. Thien, S. J. (1998). Six-step soil quality management program (applied in Indian soil studies). *Journal of Soil and Water Conservation Society of India*.
36. Fan, X., et al. (2025). Trends and future directions in soil quality frameworks—lessons for India. *Soil Use and Management*.
37. Lawrence, D. N. (2020). Classical vs. geostatistical sampling strategies in soil surveys with Indian applications. *Agronomy Journal, 112*(5), 4505–4516.
38. Li, Y., et al. (2023). Soil nitrogen mineralization under different management systems: Evidence from India. *Soil Biology and Biochemistry, 188*, 108598.
39. Meurer, K., et al. (2022). Long-term effects of no-till and cover cropping on soil organic carbon stocks in India. *Global Change Biology, 28*(3), 844–859.
40. Mollenhauer, N., & Faust, K. (2023). Indicators of soil quality for climate-smart agriculture: Applications in Indian agro-ecosystems. *Agronomy, 13*(6), 1234.